Real-time phase-shifting techniques for determining the photoelastic parameters: a theoretical comparison

Zhenkun Lei (雷振坤)[1], Yilan Kang (亢一澜)[1], and Dazhen Yun (云大真)[2]

[1] *Department of Mechanics, School of Mechanical Engineering, Tianjin University, Tianjin 300072*

[2] *Department of Engineering Mechanics, Dalian University of Technology, Dalian 116024*

Received May 19, 2003

Among data acquisition techniques in digital photoelasticity, the integrated phase shifting technique (IPST) can real-time analyze the photoelastic parameters at a video rate of the high speed CCD camera. In this paper, fourteen algorithms are described by different configurations of the rotating an analyzer at a constant rate and an output quarter-wave plate at another constant rate. The theoretical comparisons of the algorithms are given by the simulated phase distributions of the isochromatic and isoclinic parameters of the disk under two cases that the load keeps unchangeable or linearly increasing in exposure time of the camera. Then a guideline is given to alleviate the influence of the load changing with time on the IPST.

OCIS codes: 120.3940, 120.5050.

Recently, many methods in digital photoelasticity[1] combining with the digital imaging techniques have been developed quickly for the analysis of photoelastic fringe patterns, such as phase shifting[2−3], color-field phase shifting[4−5], load stepping[6−8], and so on. Many methods mentioned above cannot be used under an increasing loading condition. In order to apply these techniques to time-varying phenomena, Yoneyama[9] has proposed an integrated phase shifting technique (IPST), which provides the phase distributions of isochromatics and isoclinics at a video rate by rotating an analyzer at a constant rate and an output quarter-wave plate at a double rate of the analyzer and continuously recording images by a CCD camera, and the sequential phase shifting images whose brightness is integrated by sensors are obtained. The IPST can be used for high-speed inspection of birefringence in glass products at a video rate and will have actively developed potential in online measurement of experimental mechanics.

In this paper, we describe fourteen algorithms in IPST by the different configurations of the rotating an analyzer at a constant rate and an output quarter-wave plate at another constant rate. The phase maps and error curves of the isochromatic and isoclinic parameters of a disk are simulated under the static and increasing loadings in exposure time of the CCD camera. The simulation results show that the 13th algorithm has the best accuracy in the isochromatic or isoclinic parameters under static load condition. Several algorithms have minimum error in the isochromatics under slow increasing loadings. On the other hand, the fringe movement induced by increasing loadings influences the isoclinics clearly. Then a guideline is given to decrease the influence of the load changing with time on the IPST. For an arrangement of a general circular polariscope shown in Fig. 1, the emerging light intensity I of photoelastic fringe pattern is expressed as

$$I = I_b + \frac{I_a}{2}[1 - \sin 2(\beta - \alpha)\cos\phi + \sin 2(\theta - \gamma)\cos 2(\beta - \gamma)\sin\phi], \quad (1)$$

where I_a and I_b are the proportionality constants of the amplitude light emerging from a polarizer and the background intensity of a fringe pattern. ϕ and θ denote the phase retardation and the direction of the maximum principal stress of a specimen respectively, the symbols β and γ are the angles between a reference axis and the fast axis of an analyzer and an output quarter-wave plate respectively. When the analyzer and the output quarter-wave plate rotate at a constant rate w and $2w$ respectively, there is the following $\gamma = 2\beta$. The output signal of the brightness from the CCD camera is obtained by integrating Eq. (1) as

$$I = \int_{\beta_1}^{\beta_2} \{I_b + \frac{I_a}{2}[1 + \sin 2\beta\cos\phi + \sin 2(\theta - 2\beta)\cos 2\beta\sin\phi]\}\mathrm{d}\beta, \quad (2)$$

where β_1 and β_2 are the initial and final angles of the analyzer, respectively. If the analyzer and the output quarter-wave rotate at constant rates $\pi/6$ and $\pi/3$ rad/frame, respectively, the intensity I_1 of the first fringe pattern can be expressed by integrating Eq. (2) from 0 to $\pi/6$ as

$$I_1 = \frac{I_a}{48}(4\pi + 6\cos\phi - 7\cos 2\theta\sin\phi + 3\sqrt{3}\sin 2\theta\sin\phi) + \frac{\pi I_b}{6}. \quad (3)$$

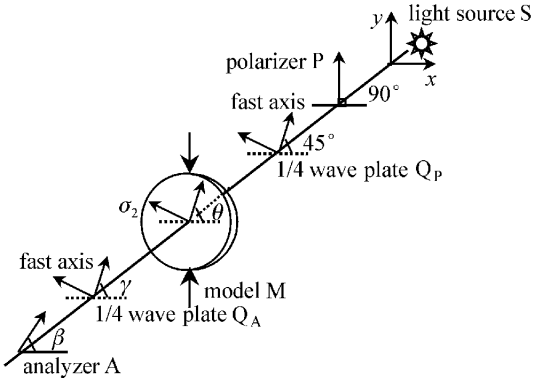

Fig. 1. General circle polariscope.

Since I_a and I_b are constants, Eq. (3) can be rewritten as

$$I_1 = \frac{I_a}{8\pi}(4\pi + 6\cos\phi - 7\cos 2\theta \sin\phi + 3\sqrt{3}\sin 2\theta \sin\phi) + I_b. \quad (4)$$

The sequential equations of the intensity $I_2, I_3 \cdots$ of the fringe pattern can be obtained in the same method. Using the six intensity values, the photoelastic parameter can be obtained

$$\tan 2\theta = \frac{2(I_1 + I_6 - I_3 - I_4)}{\sqrt{3}(I_2 + I_4 + I_6 - I_1 - I_3 - I_5)}, \quad \text{for } \sin\phi \neq 0, \quad (5)$$

$$\tan\phi = \frac{6(I_2 + I_4 + I_6 - I_1 - I_3 - I_5)}{[7(I_2 - I_5) + I_4 + I_6 - I_1 - I_3)]\cos 2\theta}, \quad \text{for } \cos 2\theta \neq 0. \quad (6)$$

The isochromatic parameter in the range of 0 to 2π and the isoclinic parameter in the range of 0 to $\pi/2$ can be obtained directly from Eqs. (5) and (6). It needs to be noted that the coefficient in the denominator of Eq. (5) in Ref. [9] is not correct.

During the acquiring of a single photoelastic image, the rotated angles of the analyzer and the output quarter-wave plate are fixed constants of $\pi/6$ and $\pi/3$ rad/frame, respectively. If the frame rate of the CCD camera is 30 frame/s, the rotating rates of the analyzer and the output quart-wave plate are $\omega = 5\pi$ rad/s and $2\omega = 10\pi$ rad/s. A series of six phase-shifted images is obtained continuously within 6/30 s. The distributions of the isochromatic and isoclinic parameters can be provided at the frame rate of the CCD camera.

Table 1. Configurations for Different Algorithms (rad/frame)

1	$\gamma = 2\beta = \pi/3$	8	$\beta = 0.5\gamma = \pi/12$
2	$\beta = 2\gamma = \pi/3$	9	$\gamma = -2\beta = -\pi/3$
3	$\gamma = 3\beta = \pi/4$	10	$\beta = -2\gamma = -\pi/3$
4	$\beta = 3\gamma = \pi/4$	11	$\gamma = -\beta = -\pi/6$
5	$\gamma = 1.5\beta = \pi/4$	12	$\beta = -\gamma = -\pi/6$
6	$\beta = 1.5\gamma = \pi/4$	13	$\gamma = -0.5\beta = -\pi/12$
7	$\gamma = 0.5\beta = \pi/12$	14	$\beta = -0.5\gamma = -\pi/12$

In fact, various algorithms of the IPST can be obtained by rotating the analyzer at a constant rate and the output quarter-wave plate at another constant rate. Table 1 summarizes the configurations of the different algorithms for different rotated angles of the analyzer and the output quarter-wave plate in an exposure time. It is assumed that a simulated disk is 50 mm diameter, 4.8 mm thickness, 7.6222 N/(mm per fringe) material fringe value and subjected to a load of 313.6 N. The frame rate of the CCD camera is $f = 30$ frame/s and the varying rate of the isochromatic parameter is $\Delta = \pi/2$ rad/s. Then the isochromatic parameter varies $\mathrm{d}\phi = \pi/60$ rad/frame at a single photoelastic image. The phase maps of photoelastic parameters calculated by the IPST 13th algorithm under the static load and increasing loadings are listed in Fig. 2. It is noted that the isochromatics close to the top and bottom areas of the disk contain incorrect regions where the isochromatic parameter has the wrong mathematical sign. It also can be seen that the

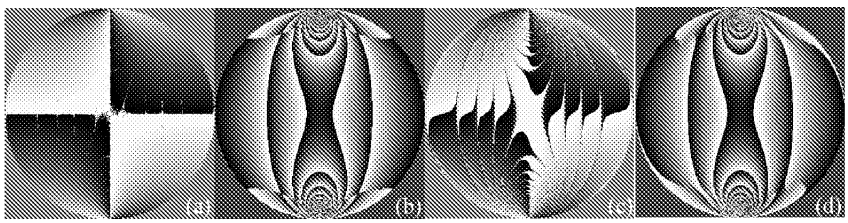

Fig. 2. Isoclinic and isochromatic phase maps calculated by the 13th IPST algorithm. (a, b) Under static load, and (c, d) under increasing load.

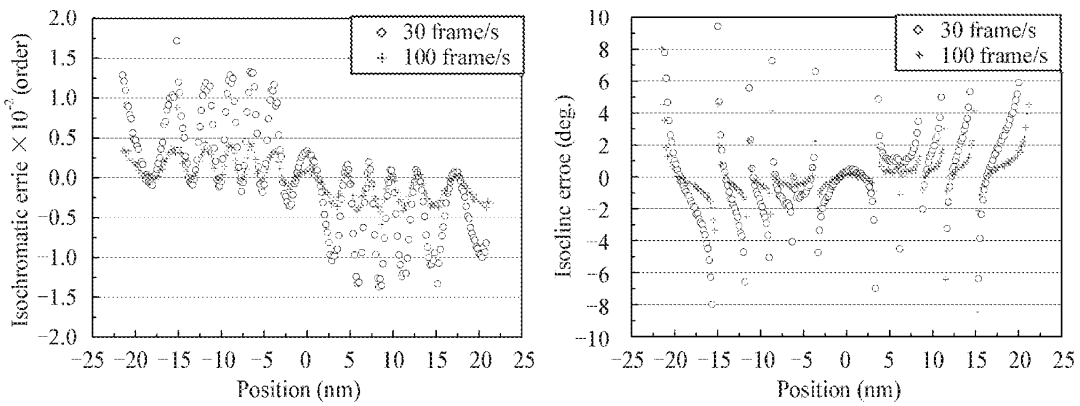

Fig. 3. Error distributions of the isoclinics and isochromatics calculated by 13th algorithm under the increasing loadings in exposure time when the frame rate of the CCD camera is 30 and 100 frame/s respectively. (a) The isochromatic error; (b) the isoclinics error.

isoclinics appear to be abnormally clear when the load is changed in exposure time.

The IPST can obtain the photoelastic parameters changing with time. However, the moving of the fringe pattern will happen due to the changing load in exposure time. For simplification, a linearly increasing loading problem is considered here. It is assumed that the isochromatic parameter varies at a constant rate during the acquisition of six images. It can be considered that this assumption is also valid for the randomly changing load if the load varies slowly. When the isochromatic parameter varies $\mathrm{d}\phi$ rad/frame at a single photoelastic image in an exposure time, Eq. (2) can be rewritten as

$$I = \int_{\phi_1}^{\phi_2} \int_{\beta_1}^{\beta_2} \{I_b + \frac{I_a}{2}[1 + \sin 2\beta \cos\phi + \sin 2(\theta - 2\beta) \cos 2\beta \sin\phi]\} \mathrm{d}\beta \mathrm{d}\phi, \quad (7)$$

where ϕ_1 and ϕ_2 are the initial and the final values of the isochromatic parameter and there is $\phi_2 - \phi_1 = \mathrm{d}\phi$. The six light intensity equations can be obtained by integrating ϕ from $\phi_0 - 3\mathrm{d}\phi$ to $\phi_0 + 3\mathrm{d}\phi$ and β from 0 to π of Eq. (7) in six exposure times. Equations (5) and (6) cannot be deduced from Eq. (7) because the six light intensity equations with the phase-shift contain different values of the isochromatic parameter. So it is inevitable that the changing load in exposure time influents the photoelastic parameters calculated by the IPST.

The absolute error distributions of the photoelastic parameters are calculated by different algorithms along a horizontal line $y = 12.5$ mm across the upper half of the disk, under the static and the increasing load. The simulated results show that the 13th algorithm has the best accuracy in the isochromatic or isoclinic parameter under a static load condition and the maximum absolute error does not exceed 0.001 fringe order in the isochromatics and 1° in the isoclinics. On the other hand, the 4th, 11th, 12th, 13th and 14th algorithms have correspondingly minimum error distributions and the most absolute error does not exceed 0.015 fringe order in the isochromatics under the slow increasing loadings. Moreover, the fringe movement induced by increasing loadings has more clear influence on the isoclinics than the isochromatics.

When the frame rate of the CCD camera f is improved from 30 to 100 frame/s, that is, the isochromatic parameter variety $\mathrm{d}\phi$ at a single image decreased from $\pi/60$ to $\pi/200$ rad/frame at a single photoelastic image, the absolute error distributions of the photoelastic parameters calculated by 13th algorithms along the horizontal line are shown in Fig. 3. The maximum error of isochromatic parameter decreases to 0.01 fringe order (Fig. 3(a)). The error of the isoclinic parameter exceeds 10°, even though the error distribution has also improved (Fig. 3(b)). The results of the simulation indicate that the IPST is not suitable to analyze the isoclinic parameter when the load is varying with time. The improvement of the frame rate of the CCD camera will alleviate the influence of the change of load during phase shifting.

Z. Lei's e-mail address is leizk@163.com.

References

1. K. Ramesh, *Digital Photoelasticity—Advanced Techniques and Applications* (Springer-Verlag, Berlin, 2000).
2. E. A. Patterson and Z. F. Wang, Strain **27,** 49 (1991).
3. K. Ramesh and V. Ganpathy, J. Strain Analysis for Eng. Des. **31,** 423 (1996).
4. G. Petrucci, Exp. Mech. **37,** 420 (1997).
5. Z. K. Lei, D. Z. Yun, and W. M. Yu, Opt. Laser Eng. **40,** 189 (2003).
6. M. J. Ekman and A. D. Nurse, Opt. Laser Eng. **36,** 1845 (1998).
7. K. Ramesh and D. K. Tamrakar, Opt. Laser Eng. **33,** 387 (2000).
8. D. K. Tamrakar and K. Ramesh, Strain **38,** 11 (2002).
9. S. Yoneyama, Y. Morimoto, and R. Matsui, Opt. Laser Eng. **39,** 1 (2003).